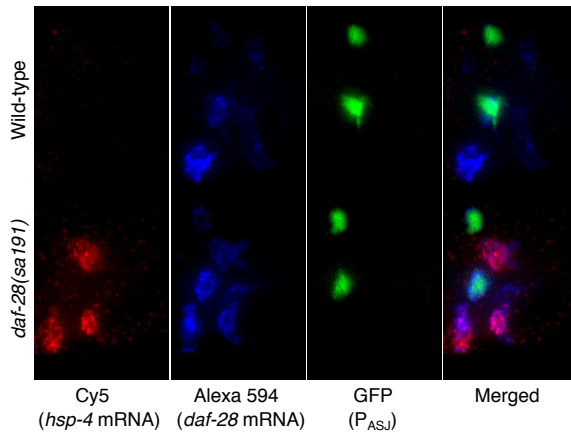
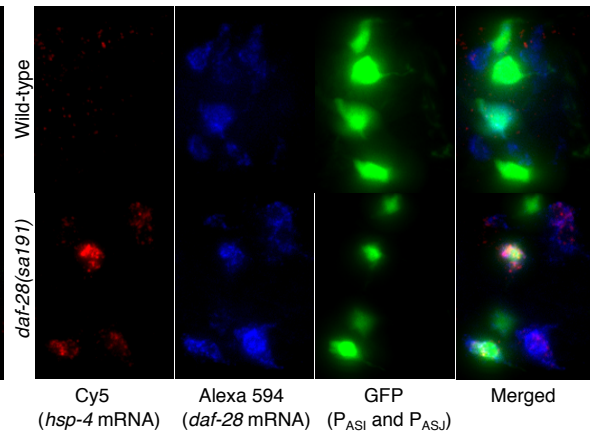
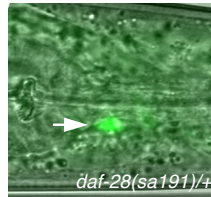
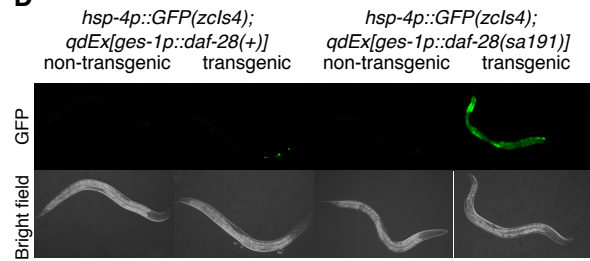
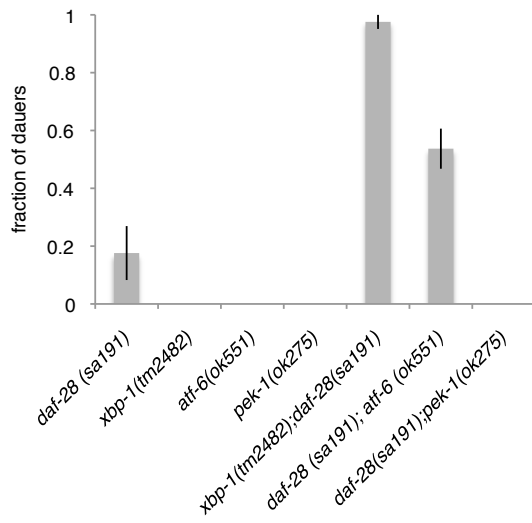


**A****B****C****D****E**

**Figure S1. The *daf-28 (sa191)* Mutation Causes ER Stress, Related to Figure 1**

(A) Maximum Z projection of smFISH stacked images of pre-dauer larvae with indicated genotypes. The ASJ neurons are identified by expression of the translational fusion TRX-1::GFP [S1].

(B) Maximum Z projection of smFISH stacked images of pre-dauer larvae with indicated genotypes. The ASI and ASJ neurons are identified by GFP expression driven by the *daf-28* promoter [S2].

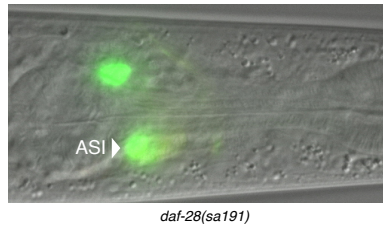
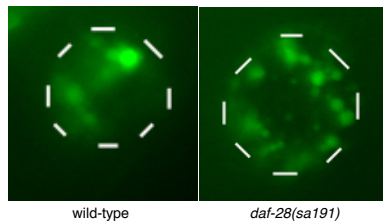
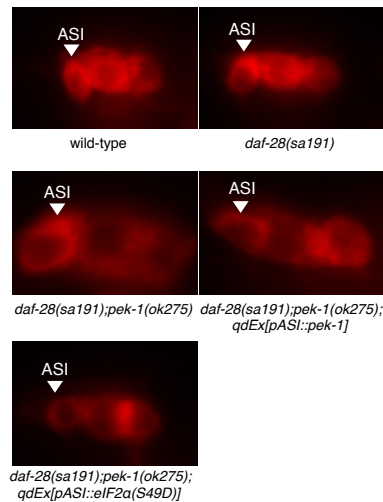
(C) Shown is fluorescence microscopy of the *daf-28(sa191)/+* heterozygote that carries the *hsp-4p::GFP* transgene (green). The filled arrow indicates ASI.

(D) Shown is fluorescence microscopy of the animals with indicated genotypes that carry the *hsp-4p::GFP* transgene. *ges-1*, an intestine-specific promoter [S3], was used to drive ectopic expression of *daf-28*, both wild-type and *sa191* versions. *ofm-1p::GFP*, expressed in the coelomocytes, was used as a visible co-injection marker for transgenic animals. All images were recorded using the same exposure time.

Images shown represent five independent transgenic lines for *qdEx[ges-1p::daf-28(sa191)]*, all of which exhibit robust induction of *hsp-4p::GFP* expression in the intestine.

For *qdEx[ges-1p::daf-28(+)]*, images shown are representative of thirteen out of fourteen independent transgenic lines. One line carrying *qdEx[ges-1p::daf-28(+)]* exhibits modest and variable induction of *hsp-4p::GFP* expression in the intestine.

(E) Fractions of the *daf-28(sa191)* mutants with indicated *xbp-1*, *atf-6* and *pek-1* deficiencies that enter the dauer stage at 20 °C. Similar results were obtained using another loss-of-function allele of *xbp-1*, *tm2457*. Plotted is mean  $\pm$  SD. The number of trials and animals scored is documented in Table S3.

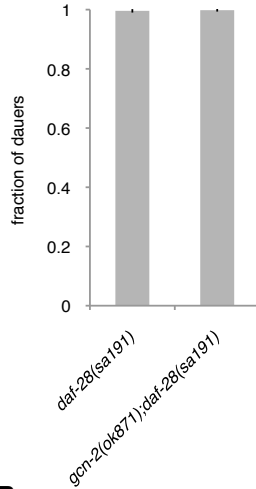
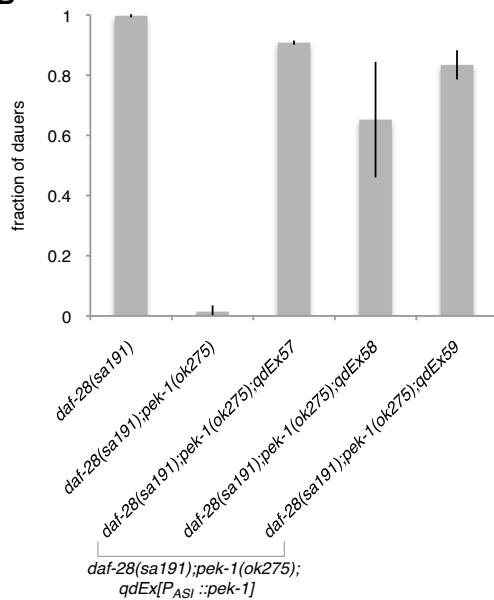
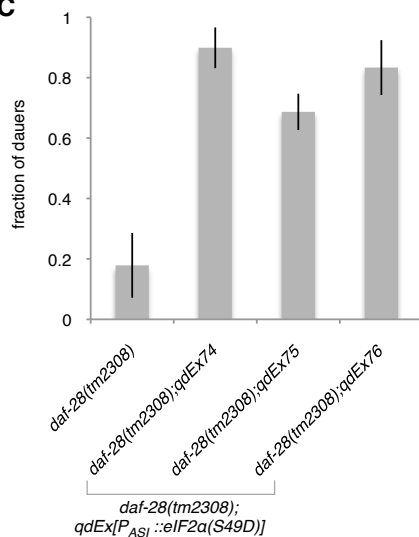
**A****B****C**

**Figure S2. The *daf-28(sa191)* Mutation and Neuronal UPR Activation Does Not Compromise Cellular Survival and Function, Related to Figure 1**

(A) Representative fluorescence microscopy of the anterior section of the *daf-28(sa191)* mutant carrying the *daf-28p::GFP* transgene. Note apparent expression of the transcriptional reporter (green).

(B) Representative fluorescence microscopy of the coelomocytes of the animals carrying the *daf-28p::DAF-28::GFP* transgene [S4] with indicated genetic backgrounds. Coelomocytes are specialized in taking up material from the pseudocoelomic fluid. Since *daf-28* is not expressed in the coelomocytes, the accumulation of DAF-28::GFP (note green puncta) could only be attributed to uptake from the pseudocoelom, where DAF-28::GFP, produced and secreted from the chemosensory neurons is deposited. The patterns depicted are representative of three independent experiments. Post-dauer animals were used in the experiments for consistency in coelomocyte identification.

(C) Fluorescence microscopy of the dye-filled amphid chemosensory neurons of the animals with indicated genotypes. The patterns depicted are representative of developmental stages both pre- and post-dauer entry at the restrictive temperature 25°C. For transgenic animals, images shown represent observations from three independent lines.

**A****B****C**

### Figure S3. PEK-1 Phosphorylates eIF2 $\alpha$ in the ASI Neuron Pair to Promote Entry into Dauer Diapause, Related to Figures 2 and 3

(A) Fractions of the animals with indicated genotypes that enter the dauer stage at 25 °C. Unlike PEK-1, GCN-2, a *C. elegans* ortholog of the eIF2 $\alpha$  kinase GCN2 that functions independently of ER stress, is not required for the constitutive entry into dauer in the *sa191* animals. These observations rule out the possibility that general dysregulation of eIF2 $\alpha$  phosphorylation promotes dauer entry, and pointing to an ER stress-specific role of PEK-1 in promoting the dauer developmental decision.

(B) Results from a second ASI-specific promoter, *str-3p*, are shown here (referred to as  $P_{ASI}$ ). The *daf-28(sa191);pek-1(ok275)* strain in this figure represents non-transgenic animals from all three lines. Both *str-3p* and *gpa-4p* were characterized and validated in previous studies [S5-S7].

(C) Fractions of the animals with indicated genotypes that enter the dauer stage at 25 °C. The *daf-28(tm2308)* strain in this figure represents non-transgenic controls from all three lines. Results from the ASI-specific *gpa-4* promoter are shown in this figure (referred to as  $P_{ASI}$ ).

Plotted is mean  $\pm$  SD. The number of trials and animals scored is documented in Table S3.

**Table S1. Data for Dauer Formation Assays, Related to Figure 1 and Discussion**

Genotype	Mean percentage of dauers $\pm$ standard deviation (percentage)	Number of trials	Number of total (pooled) animals
<i>daf-28(sa191)</i>	97.8 $\pm$ 3.9	19	1017
<i>daf-16(mgDf47);daf-3(mgDf90)</i>	0 $\pm$ 0	10	690
<i>daf-16(mgDf47);daf-28(sa191);daf-3(mgDf90)</i>	38.4 $\pm$ 10.4*	8	371

**Note:** The *daf-16(mgDf47);daf-28(sa191);daf-3(mgDf90)* animals only formed partial dauers (\*), the features of which were described in [S8]. A previous study showed that *daf-16;daf-28(sa191)* mutants only formed partial dauers, and the fraction of partial dauers was significantly lower than the fraction of *bona fide* dauers formed by the *daf-28(sa191)* mutant [S9].

**Table S2. Data for Dauer Formation Assays, Related to Figures 1, 2 and 3****Figure 1A**

Genotype	Mean percentage of dauers $\pm$ standard deviation (percentage)	Number of trials	Number of total (pooled) animals
N2	0 $\pm$ 0	7	221
<i>daf-28(gk411072)</i>	0.6 $\pm$ 0.5	6	657
<i>daf-28(tm2308)</i>	6.3 $\pm$ 4.8	19	887
<i>daf-28(gk411072)/daf-28(tm2308)</i>	0.4 $\pm$ 1.3	10	183
<i>daf-28(sa191)/daf-28(gk411072)</i>	72.5 $\pm$ 1.0	5	77
<i>daf-28(sa191)/daf-28(tm2308)</i>	83.7 $\pm$ 6.0	9	399
<i>daf-28(sa191)</i>	97.5 $\pm$ 4.0	16	857

**Note:** We observed minimal or no Daf-c phenotype in animals carrying two putative null alleles of *daf-28*, the *daf-28(tm2308)* [S10] and *daf-28(gk411072)* alleles that were not available at the time of prior studies, indicating that the robust Daf-c phenotype of the *sa191* mutant cannot be attributed to loss of function of the insulin-encoding gene *daf-28*. In addition, the trans-heterozygote between the *sa191* mutation and each of the *daf-28* null alleles exhibited constitutive entry into dauer similar to the *sa191* homozygote, corroborating the reported gain-of-function nature of the *sa191* mutation.

**Figure 2A**

Genotype	Mean percentage of dauers $\pm$ standard deviation (percentage)	Number of trials	Number of total (pooled) animals
<i>daf-28(sa191)</i>	99.7 $\pm$ 0.5	8	665
<i>daf-28(sa191);ire-1(v33)</i>	99.6 $\pm$ 1.1	7	264
<i>daf-28(sa191);xbp-1(tm2482)</i>	99.6 $\pm$ 1.0	7	357
<i>daf-28(sa191);atf-6(ok551)</i>	99.1 $\pm$ 1.4	8	595

**Figure 2B**

Genotype	Mean percentage of dauers $\pm$ standard deviation (percentage)	Number of trials	Number of total (pooled) animals
<i>daf-28(sa191)</i>	99.7 $\pm$ 0.5	8	665
<i>daf-28(sa191);pek-1(ok275)</i>	1.9 $\pm$ 2.8	9	891
<i>daf-28(sa191);pek-1(tm629)</i>	0.9 $\pm$ 1.2	6	456

**Figure 2C**

Genotype	Mean percentage of dauers $\pm$ standard deviation (percentage)	Number of trials	Number of total (pooled) animals
N2	0 $\pm$ 0	8	264
<i>pek-1(ok275)</i>	0 $\pm$ 0	7	537
<i>daf-2(e1368)</i>	96.8 $\pm$ 3.5	7	325
<i>daf-2(e1368);pek-1(ok275)</i>	100 $\pm$ 0	4	237
<i>daf-7(ok3125)</i>	100 $\pm$ 0	2	97
<i>daf-7(ok3125);pek-1(ok275)</i>	97.8 $\pm$ 1.5	6	411

**Figure 2D**

Genotype	Mean percentage of dauers $\pm$ standard deviation (percentage)	Number of trials	Number of total (pooled) animals
<i>daf-28(sa191)</i>	99.7 $\pm$ 0.5	8	665
<i>daf-28(sa191);pek-1(ok275)</i>	4.4 $\pm$ 3.45	12	542
<i>daf-28(sa191);pek-1(ok275);qdEx48</i>	82.8 $\pm$ 3.9	4	103
<i>daf-28(sa191);pek-1(ok275);qdEx49</i>	85.9 $\pm$ 6.4	4	194
<i>daf-28(sa191);pek-1(ok275);qdEx50</i>	91.9 $\pm$ 5.0	4	278

**Figure 3A**

Genotype	Mean percentage of dauers $\pm$ standard deviation (percentage)	Number of trials	Number of total (pooled) animals
<i>daf-28(sa191)</i>	94.1 $\pm$ 5.1	13	399
<i>daf-28(sa191);qdEx51</i>	73.1 $\pm$ 3.6	4	141
<i>daf-28(sa191);qdEx52</i>	67.9 $\pm$ 7.6	4	169
<i>daf-28(sa191);qdEx53</i>	54.8 $\pm$ 11.4	4	119

**Figure 3B**

Genotype	Mean percentage of dauers $\pm$ standard deviation (percentage)	Number of trials	Number of total (pooled) animals
<i>daf-28(sa191);pek-1(ok275)</i>	2.4 $\pm$ 2.0	14	1037
<i>daf-28(sa191);pek-1(ok275);qdEx54</i>	69.9 $\pm$ 1.4	5	254
<i>daf-28(sa191);pek-1(ok275);qdEx55</i>	91.5 $\pm$ 8.0	5	117

**Table S3. Data for Dauer Formation Assays, Related to Figures 3, S1, S2 and S3 and Discussion****Related to Figure 3**

Genotype	Mean percentage of dauers $\pm$ standard deviation (percentage)	Number of trials	Number of total (pooled) animals
<i>daf-28(sa191)</i>	98.3 $\pm$ 2.4	10	536
<i>daf-28(sa191);qdEx60</i>	98.1 $\pm$ 1.3	4	139
<i>daf-28(sa191);qdEx61</i>	98.4 $\pm$ 1.4	3	135
<i>daf-28(sa191);qdEx62</i>	98.3 $\pm$ 2.9	3	54
<i>daf-28(sa191);pek-1(ok275)</i>	0.1 $\pm$ 0.4	12	612
<i>daf-28(sa191);pek-1(ok275);qdEx71</i>	0.4 $\pm$ 0.8	4	196
<i>daf-28(sa191);pek-1(ok275);qdEx72</i>	0 $\pm$ 0	4	118
<i>daf-28(sa191);pek-1(ok275);qdEx73</i>	0 $\pm$ 0	4	156

**Note:** *qdEx60*, *qdEx61*, *qdEx62*, *qdEx71*, *qdEx72* and *qdEx73* represent *qdEx[gpa-4p::eIF2 $\alpha$ (+):unc-54 3'UTR]*.

**Figure S1E**

Genotype	Mean percentage of dauers $\pm$ standard deviation (percentage) at 20 °C	Number of trials	Number of total (pooled) animals
<i>daf-28(sa191)</i>	17.6 $\pm$ 9.3	7	511
<i>xbp-1(tm2482)</i>	0 $\pm$ 0	4	228
<i>atf-6(ok551)</i>	0 $\pm$ 0	4	280
<i>pek-1(ok275)</i>	0 $\pm$ 0	4	274
<i>xbp-1(tm2482);daf-28(sa191)</i>	97.6 $\pm$ 2.4	5	228
<i>daf-28(sa191);atf-6(ok551)</i>	53.7 $\pm$ 6.9	6	280
<i>daf-28(sa191);pek-1(ok275)</i>	0 $\pm$ 0	6	304

**Figure S3A**

Genotype	Mean percentage of dauers $\pm$ standard deviation (percentage)	Number of trials	Number of total (pooled) animals
<i>daf-28(sa191)</i>	99.6 $\pm$ 0.6	8	659
<i>gcn-2(ok871);daf-28(sa191)</i>	99.8 $\pm$ 0.5	6	427

**Figure S3B**

Genotype	Mean percentage of dauers $\pm$ standard deviation (percentage)	Number of trials	Number of total (pooled) animals
<i>daf-28(sa191)</i>	99.7 $\pm$ 0.5	8	665
<i>daf-28(sa191);pek-1(ok275)</i>	1.4 $\pm$ 2.0	12	591
<i>daf-28(sa191);pek-1(ok275);qdEx57</i>	90.8 $\pm$ 0.7	4	121
<i>daf-28(sa191);pek-1(ok275);qdEx58</i>	65.2 $\pm$ 19.2	4	102
<i>daf-28(sa191);pek-1(ok275);qdEx59</i>	83.4 $\pm$ 4.8	4	246



**Figure S3C**

Genotype	Mean percentage of dauers $\pm$ standard deviation (percentage)	Number of trials	Number of total (pooled) animals
<i>daf-28(tm2308)</i>	17.9 $\pm$ 10.7	14	412
<i>daf-28(tm2308);qdEx74</i>	89.9 $\pm$ 6.7	5	154
<i>daf-28(tm2308);qdEx75</i>	68.7 $\pm$ 6.0	4	146
<i>daf-28(tm2308);qdEx76</i>	83.3 $\pm$ 9.1	5	122

**Related to Figure S2 and Discussion**

Genotype	Mean percentage of dauers $\pm$ standard deviation (percentage)	Number of trials	Number of total (pooled) animals
<i>daf-28(sa191)</i>	99.6 $\pm$ 0.6	6	493
<i>daf-28(sa191);daf-3(mgDf90)</i>	99.8 $\pm$ 0.5	6	564

**Note:** DAF-3/SMAD is required for chemosensory neuron ablation to mediate dauer formation [S11]. The result is consistent with a previous genetic study [S9] using a different allele of *daf-3*, namely *e1376*.

## Supplemental Experimental Procedures

### *Caenorhabditis elegans* Strains

Additional strains were used in Figures S1, S2 and S3 and Tables S1, S2 and S3: GR1455 *mgIs40[daf-28p::GFP]*, ZD803 *daf-28(sa191);mgIs40[daf-28p::GFP]*, OE3010 *ofEx4[trx-1p::TRX-1::GFP]*, ZD1065 *daf-28(sa191);ofEx4[trx-1p::TRX-1::GFP]*, ZD747 *svIs69[daf-28p::DAF-28::GFP]*, ZD805 *daf-28(sa191);svIs69[daf-28p::DAF-28::GFP]*, ZD1066-1068 *zcIs4[hsp-4p::GFP];qdEx80-82[ges-1p::daf-28(+):unc-54 3'UTR]*, ZD1069-1071 *zcIs4[hsp-4p::GFP];qdEx80-82[ges-1p::daf-28(sa191):unc-54 3'UTR]* ZD815 *gcn-2(ok871);daf-28(sa191)*, ZD954-956 *daf-28(sa191);pek-1(ok275);qdEx57-59[str-3p::pek-1::unc-54 3'UTR]*, ZD933, 1021 and 1023 *daf-28(tm2308);qdEx74-76[gpa-4p::eIF2 $\alpha$ (S49D)::unc-54 3'UTR]*, ZD967-969 *daf-28(sa191);qdEx60-62[gpa-4p::eIF2 $\alpha$ (WT)::unc-54 3'UTR]*, ZD995-997 *daf-28(sa191);pek-1(ok275);qdEx71-73[gpa-4p::eIF2 $\alpha$ (WT)::unc-54 3'UTR]*, GR1311 *daf-3(mgDf90)*, ZD822 *daf-28(sa191);daf-3(mgDf90)*, ZD939 *daf-16(mgDf47);daf-28(sa191);daf-3(mgDf90)* and ZD941 *daf-16(mgDf47);daf-3(mgDf90)*.

The strain carrying *daf-28(tm2308)* allele was kindly provided by G. Ruvkun. The strain carrying *pek-1(ok275)* was kindly provided by M. Crowder. The strain carrying *svIs69* was kindly provided by S. Tuck. Unless otherwise noted, the ZD strains have been outcrossed at least three times. ZD940 was outcrossed twice. Strains carrying the *pek-1(tm629)* and *atf-6(ok551)* alleles were outcrossed once to the *daf-28(sa191)* strain. In addition to using two independent alleles of *pek-1*, the transheterozygote between the *pek-1(ok275)* and *pek-1(tm629)* alleles was generated in the *sa191* background to confirm the suppression of the Daf-c phenotype by *pek-1* loss-of-function mutations. Double and triple mutants were generated and genotyped using standard methods (relying on PCR or visible phenotypes, when

possible). Experiments involving transheterozygotes were performed by crossing the two indicated strains. The mated P<sub>0</sub> hermaphrodites were allowed to lay eggs under the same condition as the original strains, and the F<sub>1</sub> cross progeny was confirmed and scored as L4 or dauer. The *daf-28(sa191)/daf-28(gk411072)* and *daf-28(tm2308)/daf-28(gk411072)* heterozygotes were derived from crosses involving the strain VC30082, carrying the *daf-28(gk411072)* allele.

### Constructs and Generation of Transgenic Lines

The *gpa-4p::pek-1::unc-54 3'UTR* construct includes 2.9 kb of *gpa-4* promoter, 4.2 kb of *pek-1* genomic region (including short introns) and 0.7 kb of *unc-54 3'UTR*. The *gpa-4* promoter region was amplified by using 5' primer 5'-ATCACACCGTCGTGAGCTA-3' and 3' primer 5'-CTATATAATACACACTCATTGTTGAAAAGTGTTACAAAATG-3' (contains an overhang complementary to the *pek-1* genomic region for subsequent PCR fusion). The *pek-1* genomic region was amplified by using 5' primer 5'-ATGAGTGTGTATTATATAG-3' and 3' primer 5'-AGGCACGGGCGCGAGATGTTATTGGAGAAATTTATGAG-3' (contains an overhang complementary to the *unc-54 3'UTR* region for subsequent PCR fusion). The *unc-54 3'UTR* region was amplified by using 5' primer 5'-CATCTCGCGCCCGTGCCT-3' and 3' primer 5'-AAGGGCCCGTACGGCCGACTAGTAGG-3'. Nested primers were used in subsequent PCR fusion, as previously described [S12]. The *str-3p::pek-1::unc-54 3'UTR* construct includes 2.9 kb of *str-3* promoter, 4.2 kb of *pek-1* genomic region (including short introns) and 0.7 kb of *unc-54 3'UTR*. The *str-3* promoter region was amplified by using 5' primer 5'-TTCAGAAGGCAGATGCAAAA-3' and 3' primer 5'-TAAAACTATATAATACACACTCATGTTTCCTTTTGAATTGAGGCAGT-3' (contains an overhang complementary to the *pek-1* genomic region for subsequent PCR fusion). The *str-3p::pek-1::unc-54 3'UTR* construct was injected at 40 ng/μl.

The *gpa-4p::eIF2α::unc-54 3'UTR* construct includes 2.9 kb of *gpa-4* promoter, 1.1 kb of *eIF2α* cDNA (wild-type, phosphomimetic and unphosphorylatable versions [S13] kindly provided by S.Takagi) and 0.7 kb of *unc-54 3'UTR*. The *gpa-4* promoter and *unc-54 3'UTR* regions were amplified as described above. The 3' primers used to amplify *gpa-4p* contain an overhang complementary to the *eIF2α* cDNA region for subsequent PCR fusion. An indicated version of *eIF2α* was amplified by using 5' primer 5'-ATGAAATGCCGTTTCTACGAG-3' and 3' primer 5'-AGGCACGGGCGCGAGATGTT AATCATCCTCCTCATCACTGT-3' (contains an overhang complementary to the *unc-54 3'UTR* region for subsequent PCR fusion). Nested primers were used in subsequent PCR fusion, as previously described.

The *ges-1p::daf-28::unc-54 3'UTR* construct includes 1.5 kb of *ges-1* promoter, 0.7 kb of *daf-28* genomic region (including an intron) and 0.7 kb of *unc-54 3'UTR*. The *ges-1* promoter region was amplified by using 5' primer 5'-CTTCGGGCGCTACCAATAAG-3' and 3' primer 5'-GATGGCGATG AGCTTGCAGTTCATCTGAATTCAAAGATAAGATATGT-3' (contains an overhang complementary to the *daf-28* genomic region for subsequent PCR fusion). The *daf-28* genomic region (wild-type and *sal191* versions) was amplified by using 5' primer 5'-TCTCCTCTCAACA ACT ATCTCAACA-3' and 3' primer 5'-AGTCAGAGGCACGGGCGCGAGATGTTAAAGAAGCAAACGTGGGCAA-3' (contains an overhang complementary to the *unc-54 3'UTR* region for subsequent PCR fusion). Nested primers were used in subsequent PCR fusion, as previously described. The *ges-1p::daf-28::unc-54 3'UTR* construct was injected at 50 ng/μl.

### **Dauer Assay**

For dauer assays involving transgenic strains, gravid extrachromosomal-array-carrying hermaphrodites were used for egg lay, and both non-transgenic and transgenic offspring were scored as

dauer or L4. Fractions of dauers were then derived for both non-transgenic and transgenic cohorts. Paired Student's t-test analyses between transgenic and non-transgenic dauer fractions from each trial were conducted for all lines. At least three independent lines were tested for each transgenic construct.

## **Microscopy**

DiI stock was diluted in M9 to the final concentration of 10 µg/ml. Worms raised at 22.5 °C or 25°C were transferred to the solution and incubated at room temperature for two hours before imaging. Rhodamine filter was used for imaging and the fluorescence signals were recorded without saturation. For the purpose of neuron identification by dye filling, both pre-dauer and post-dauer animals were mounted. Dauer animals were not used for this purpose because some amphid neurons are altered in shape and position in the dauer stage [S14].

## **Single Molecule Fluorescent *in situ* Hybridization (smFISH)**

smFISH was performed as described previously [S15]. Pre-dauer larvae grown at 25°C were used in the experiments. *hsp-4* probes were coupled to Cy5 and *daf-28* probes were coupled to Alexa Fluor 594. The oligonucleotide probes were designed based on the coding sequences of *hsp-4* and *daf-28*, using Stellaris FISH probe designer. To ensure specificity, *hsp-4* probes were designed to target the deleted region of the *hsp-4(gk514)* allele, and the probes yielded detectable signals in wild-type animals, but not in the *hsp-4(gk514)* mutant (data not shown). The same strategy could not be adopted for *daf-28* probe design because the deleted region of the only deletion allele of *daf-28* available (*tm2308*) is too small. The designed *daf-28* probes allowed us to detect *daf-28* mRNA in the ASI and ASJ neurons, corroborating observations from previous studies using GFP transcriptional and translational reporters [S2, S4]. Note, however, that *daf-28* mRNA expression levels are lower in ASJ (Figures S1A and S1B).

Hybridized larvae were imaged using a Nikon Ti-E inverted fluorescence microscope equipped with a 100x oil-immersion objective and a Photometrics Pixis 1024 CCD camera using MetaMorph software and appropriate optical filters for Cy5, Alexa Fluor 594 and GFP. At least 10-20 animals per genotype were examined, and the observed *daf-28* and *hsp-4* mRNA expression patterns were derived from at least three independent experiments. ImageJ was used to perform maximum Z projection of stacked images. For image presentation, only linear adjustment (brightness and contrast) was applied equally to images from different genotypes to optimize signal-to-noise ratios for each channel.

## Supplemental References

1. Miranda-Vizuete, A., Fierro Gonzalez, J.C., Gahmon, G., Burghoorn, J., Navas, P., and Swoboda, P. (2006). Lifespan decrease in a *Caenorhabditis elegans* mutant lacking TRX-1, a thioredoxin expressed in ASJ sensory neurons. *FEBS Lett* *580*, 484-490.
2. Li, W., Kennedy, S.G., and Ruvkun, G. (2003). *daf-28* encodes a *C. elegans* insulin superfamily member that is regulated by environmental cues and acts in the DAF-2 signaling pathway. *Genes Dev* *17*, 844-858.
3. Urano, F., Calfon, M., Yoneda, T., Yun, C., Kiraly, M., Clark, S.G., and Ron, D. (2002). A survival pathway for *Caenorhabditis elegans* with a blocked unfolded protein response. *J Cell Biol* *158*, 639-646.
4. Kao, G., Nordenson, C., Still, M., Ronnlund, A., Tuck, S., and Naredi, P. (2007). ASNA-1 positively regulates insulin secretion in *C. elegans* and mammalian cells. *Cell* *128*, 577-587.
5. Bishop, N.A., and Guarente, L. (2007). Two neurons mediate diet-restriction-induced longevity in *C. elegans*. *Nature* *447*, 545-549.
6. Jansen, G., Thijssen, K.L., Werner, P., van der Horst, M., Hazendonk, E., and Plasterk, R.H. (1999). The complete family of genes encoding G proteins of *Caenorhabditis elegans*. *Nat Genet* *21*, 414-419.
7. Park, D., Jones, K.L., Lee, H., Snutch, T.P., Taubert, S., and Riddle, D.L. (2012). Repression of a potassium channel by nuclear hormone receptor and TGF-beta signaling modulates insulin signaling in *Caenorhabditis elegans*. *PLoS Genet* *8*, e1002519.
8. Vowels, J.J., and Thomas, J.H. (1992). Genetic analysis of chemosensory control of dauer formation in *Caenorhabditis elegans*. *Genetics* *130*, 105-123.
9. Malone, E.A., Inoue, T., and Thomas, J.H. (1996). Genetic analysis of the roles of *daf-28* and *age-1* in regulating *Caenorhabditis elegans* dauer formation. *Genetics* *143*, 1193-1205.
10. Cornils, A., Gloeck, M., Chen, Z., Zhang, Y., and Alcedo, J. (2011). Specific insulin-like peptides encode sensory information to regulate distinct developmental processes. *Development* *138*, 1183-1193.
11. Bargmann, C.I., and Horvitz, H.R. (1991). Control of larval development by chemosensory neurons in *Caenorhabditis elegans*. *Science* *251*, 1243-1246.
12. Hobert, O. (2002). PCR fusion-based approach to create reporter gene constructs for expression analysis in transgenic *C. elegans*. *Biotechniques* *32*, 728-730.
13. Nukazuka, A., Fujisawa, H., Inada, T., Oda, Y., and Takagi, S. (2008). Semaphorin controls epidermal morphogenesis by stimulating mRNA translation via eIF2alpha in *Caenorhabditis elegans*. *Genes Dev* *22*, 1025-1036.

14. Albert, P.S., and Riddle, D.L. (1983). Developmental alterations in sensory neuroanatomy of the *Caenorhabditis elegans* dauer larva. *J Comp Neurol* 219, 461-481.
15. Raj, A., van den Bogaard, P., Rifkin, S.A., van Oudenaarden, A., and Tyagi, S. (2008). Imaging individual mRNA molecules using multiple singly labeled probes. *Nat Methods* 5, 877-879.